

Topological solitons stabilized by a background gauge field and soliton-anti-soliton asymmetry

Yuki Amari,^{a,b} Minoru Eto,^{c,a,d} Muneto Nitta^{b,a,d}

^a*Research and Education Center for Natural Sciences, Keio University, 4-1-1 Hiyoshi, Yokohama, Kanagawa 223-8521, Japan*

^b*Department of Physics, Keio University, 4-1-1 Hiyoshi, Yokohama, Kanagawa 223-8521, Japan*

^c*Department of Physics, Yamagata University, Kojirakawa-machi 1-4-12, Yamagata, Yamagata 990-8560, Japan*

^d*International Institute for Sustainability with Knotted Chiral Meta Matter (SKCM²), Hiroshima University, 1-3-2 Kagamiyama, Higashi-Hiroshima, Hiroshima 739-8511, Japan*

E-mail: amari.yuki@keio.jp, meto@sci.kj.yamagata-u.ac.jp,
nitta@phys-h.keio.ac.jp

ABSTRACT: We study topological lumps supported by the second homotopy group $\pi_2(S^2) \simeq \mathbb{Z}$ in a gauged $O(3)$ model without any potential term coupled with a (non)dynamical $U(1)$ gauge field. It is known that gauged-lumps are stable with an easy-plane potential term but are unstable to expand if the model has no potential term. In this paper, we find that these gauged lumps without a potential term can be made stable by putting them in a uniform magnetic field, irrespective of whether the gauge field is dynamical or not. In the case of the non-dynamical gauge field, only either of lumps or anti-lumps stably exists depending on the sign of the background magnetic field, and the other is unstable to shrink to be singular. We also construct coaxial multiple lumps whose size and mass exhibit a behaviour of droplets. In the case of the dynamical gauge field, both the lumps and anti-lumps stably exist with different masses; the lighter (heavier) one corresponds to the (un)stable one in the case of the nondynamical gauge field. We find that a lump behaves as a superconducting ring and traps magnetic field in its inside, with the total magnetic field reduced from the background magnetic field.

Contents

1	Introduction	1
2	Gauged lumps with nondynamical gauge field in a constant magnetic field background	3
2.1	The $U(1)$ gauged $\mathbb{C}P^1$ model	4
2.2	Derrick's theorem	4
2.3	$k = \pm 1$ lump solution and the selecting rule	6
2.4	Coaxial multiple lumps	9
3	Gauged lumps with dynamical gauge field in a magnetic field background	9
3.1	The model with dynamical gauge field	10
3.2	Derrick's theorem	10
3.3	Multiple gauged lumps in the down vacuum with $eB > 0$	12
3.4	Gauged anti-lumps in the down vacuum with $eB > 0$	16
4	Summary and discussion	17
A	A BPS lump for $B = 0$	19

1 Introduction

Solitons are non-perturbative excitations playing significant roles in physics and mathematics. In particular, topological solitons are protected by topology and thus are quite stable, ubiquitously appearing in quantum field theory [1–11], cosmology [12–16] and condensed matter systems [17–21]. Topological solitons are classified into defects and textures, the both of which are characterized by homotopy groups in a different fashion. The former contains domain walls, vortices and monopoles, while the latter does sine-Gordon solitons, baby(2D) Skyrmons, and Skyrmons. However, topology is not sufficient for the stability of solitons; energetically they may prefer to shrink or expand without suitable settings. The Derrick's scaling argument offers a simple criterion of the stability under scaling of solitons of finite energy [22]. For instance, in $d = 3 + 1$ dimensions, Skyrmons [23, 24] and Hopfions [25–27] are unstable to shrink without a four derivative Skyrme term. In $d = 2 + 1$ dimensions, topological lumps (equivalently sigma model instantons in 2+0 dimensions) are scale invariant [28], while they shrink in the presence of a potential term, which can be prevented by introducing a four-derivative Skyrme term as baby Skyrmons [29–32] or time dependence as Q-lumps [33, 34]. Vortices can be made finite energy by introducing gauge field, otherwise they have infinite energy.

Here, we pursue a yet another possibility for the stabilization of topological solitons in terms of a background field. Topological solitons unstable to shrink or expand can be prevented from collapsing by a background field. In fact, such a stabilization mechanism is well known in condensed matter physics as far as background fields are not dynamical, while our target is the case of dynamical fields with backgrounds; In condensed matter physics, a typical example with nondynamical background field is given by magnetic Skyrmions [35–43], that is 2D Skyrmions in chiral magnets, which are stable even without a four derivative Skyrme term. Chiral magnets are described by the CP^1 model with a so-called Dzyaloshinskii-Moriya (DM) interaction [44, 45] which prevents Skyrmions from shrinking. This interaction can be reformulated as a background $SU(2)$ gauge field (a constant $SU(2)$ magnetic field) [43, 46]. See e.g. Refs. [43, 47] for a Derrick’s scaling argument. One of characteristic features is that only Skyrmions are stable while anti-Skyrmions are unstable to shrink. Magnetic Skyrmions have been generalized to CP^2 Skyrmions [48, 49]. Ultracold atomic gases with spin-orbit couplings or synthetic gauge fields [50, 51] offer various examples such as 2D Skyrmions [52] and 3D Skyrmions [53]. As mentioned above, in all condensed matter examples, a gauge field is nondynamical and thus is a constant background field.

Let us illustrate our idea with taking a concrete example of topological lumps (or sigma model instantons in $d = 2 + 0$) supported by the second homotopy group $\pi_2(S^2) \simeq \mathbb{Z}$ in an $O(3)$ model or equivalently CP^1 model in $d = 2 + 1$ dimensions [28]. Topological lumps are scale invariant solutions in the CP^1 model without a potential. The structure of topological lumps becomes completely different if we gauge an $SO(2) \simeq U(1)$ subgroup of $O(3)$. The $U(1)$ gauged CP^1 model with an easy-plane potential term is known to admit stable lumps [54–57], where a lump is decomposed into a pair of a vortex and anti-vortex with fractional lump charges (sometimes called merons). However, if there is no potential term, lumps are unstable to expand and eventually diluted.

In this paper, we show that these gauged-lumps without potentials can be made stable if we put them in a uniform magnetic field background. We separately consider the cases that the $U(1)$ gauge field is nondynamical and dynamical, and construct topological lump solutions in the presence of a uniform magnetic field background. In the both cases, we apply the Derrick’s scaling argument, numerically solve the equations of motion (EOM) for the axisymmetric lumps, and confirm the Derrick’s scaling argument within numerical accuracy. One of interesting results peculiar to our models with the background magnetic field is asymmetry between solitons and anti-solitons; In the case of the non-dynamical gauge field, either of lumps or anti-lumps stably exists depending on the sign of the background magnetic field, and the other is unstable to shrink to a singular configuration. This situation is quite analogous to magnetic Skyrmions in chiral magnets. We find that the stable (anti-)lumps have no size modulus reflecting the fact that the model is not scale invariant due to the mass scale \sqrt{eB} with the background magnetic field B and $U(1)$ gauge coupling constant e . We numerically find that the lump size is of order $1/\sqrt{eB}$ and asymptotic tails of profile functions decay to the vacuum exponentially, unlike ungauged BPS lumps whose profiles decay polynomially. The mass of the single lump is smaller than that of a BPS lump. We also construct coaxial lumps with higher winding number k and find

that their size and mass are proportional to \sqrt{k} up to a constant shift, implying that the lumps behave as droplets. The higher lumps exhibit ring-like shape and their interiors are empty. On the other hand, in the case of the dynamical gauge field, the above properties of the stable lumps for the non-dynamical gauge field remain qualitatively correct. However, unlike the nondynamical case, both the lumps and anti-lumps stably exist as regular solutions with different masses; the lighter one corresponds to the regular one in the case of the nondynamical gauge field, while the heavier one does to the unstable (singular) one. The dynamical gauge field deforms the magnetic field around the lumps. We find that a lump behaves as a superconducting ring and traps magnetic field in its inside, with the total magnetic field reduced from the background magnetic field because of superconductivity expelling it. The higher lumps appear as ring-like shape but their interiors are not empty and are filled by trapped magnetic fields which are almost constant.

A motivation to consider the problem of this paper is originated from QCD in the presence of strong magnetic fields. QCD phase structure with a finite chemical potential in the presence of strong magnetic fields gather a lot of attention due to its relevance in neutron stars and heavy-ion collisions [58–63]. When a magnetic field and/or chemical potential is large enough, a neutral pion π^0 domain wall or soliton has a negative tension due to the anomalous term [64] when it is perpendicular to the magnetic field [65]. Thus, domain walls are spontaneously created in such a region, and the ground state is a stack of the domain walls, called a chiral soliton lattice (CSL) [66, 67]. However, it has been recently found that a large part of CSL with stronger magnetic field and larger baryon density should be replaced by a new phase, the domain-wall Skyrmion phase [68, 69] (see also Ref. [70] for a counterpart under rapid rotation), where topological lumps supported by $\pi_2(S^2) \simeq \mathbb{Z}$ have negative energy and spontaneously appear inside a soliton [71–73]. To conclude this result, the effective theory on a single soliton was used, which is nothing but a $d = 2 + 1$ dimensional $U(1)$ gauged $\mathbb{C}P^1$ model without a potential in a constant magnetic field background. In the previous studies [68–70], we have used conventional BPS lumps by neglecting the electromagnetic interaction as an approximation. However, they should be replaced by gauged lumps constructed in this paper that may improve the phase boundary between the CSL and domain-wall Skyrmion phase.

This paper is organized as follows. In Sec. 2, we construct gauged lumps with non-dynamical gauge field in a constant magnetic field background. In Sec. 3, we consider dynamical gauge field and find that gauged lump solutions remain stable. Sec. 4 is devoted to a summary and discussion.

2 Gauged lumps with nondynamical gauge field in a constant magnetic field background

In this section, we consider nondynamical constant background gauge field. In Sec. 2.1, we briefly explain the gauged $\mathbb{C}P^1$ model. Then we explain the Derrick’s theorem in Sec. 2.2, and show the numerical solutions for the single lump in Sec. 2.3 and for the higher charged lumps in Sec. 2.4.

2.1 The $U(1)$ gauged $\mathbb{C}P^1$ model

We consider a $U(1)$ gauged $O(3)$ model or equivalently $\mathbb{C}P^1$ model in $2 + 1$ dimensions. The Lagrangian is given by

$$\mathcal{L} = -\frac{1}{4}F_{\mu\nu}F^{\mu\nu} + D_\mu\vec{n} \cdot D^\mu\vec{n}, \quad (2.1)$$

where \vec{n} is a three-component real column vector of scalar fields with the S^2 constraint

$$\vec{n} = \begin{pmatrix} n_1 \\ n_2 \\ n_3 \end{pmatrix}, \quad \vec{n}^2 = v^2, \quad (2.2)$$

where v is a radius of S^2 whose mass dimension is $\frac{1}{2}$. We gauge the $SO(2)$ symmetry about the n_3 -axis as

$$n_1 + in_2 \rightarrow e^{-i\theta(x)}(n_1 + in_2), \quad n_3 \rightarrow n_3, \quad (2.3)$$

with the covariant derivatives

$$D_\mu n_1 = \partial_\mu n_1 + eA_\mu n_2, \quad D_\mu n_2 = \partial_\mu n_2 - eA_\mu n_1, \quad D_\mu n_3 = \partial_\mu n_3. \quad (2.4)$$

Here, A_μ is the $U(1)$ gauge field and e is the $U(1)$ gauge coupling constant. This can be also expressed as $D_\mu(n_1 + in_2) = (\partial_\mu - ieA_\mu)(n_1 + in_2)$ with $A_\mu \rightarrow A_\mu - \partial_\mu\theta/e$. The mass dimensions are summarised as $[\vec{n}] = [v] = \frac{1}{2}$, $[A_\mu] = \frac{1}{2}$, and $[e] = \frac{1}{2}$. The symmetry of the model is $U(1) \times \mathbb{Z}_2$ where the \mathbb{Z}_2 is $n_3 \rightarrow -n_3$.

In the rest of this section we will consider a constant magnetic field background $F_{12} = B$, where the gauge field is not dynamical. In order to distinguish the nondynamical background gauge field from a dynamical one, we will use \mathcal{A}_μ for the former. Hereafter, we will take

$$\mathcal{A}_0 = 0, \quad \mathcal{A}_1 = -\frac{By}{2}, \quad \mathcal{A}_2 = \frac{Bx}{2}. \quad (2.5)$$

2.2 Derrick's theorem

We will study the topological lump solutions for $B \neq 0$ below. The static energy of the scalar field in the temporal gauge $\mathcal{A}_0 = 0$ is given by

$$E[\vec{n}] = \int d^2x |D_i\vec{n}|^2 = \int d^2x [|\partial_i\vec{n}|^2 + 2e\mathcal{A}_i\epsilon_{ab}\partial_in_an_b + e^2\mathcal{A}_i^2(n_1^2 + n_2^2)]. \quad (2.6)$$

Here we remove infinite energy of the constant magnetic field, so that $E[\vec{n}]$ can be finite. We now want to apply the Derrick's scaling argument to $E[\vec{n}]$. For this purpose, we divide the energy into three pieces as

$$E = E_2 + E_1 + E_0 \quad (2.7)$$

with

$$E_2 = \int d^2x |\partial_i \vec{n}|^2, \quad (2.8)$$

$$E_1 = \int d^2x 2e \mathcal{A}_i \varepsilon_{ab} (\partial_i n_a) n_b, \quad (2.9)$$

$$E_0 = \int d^2x e^2 \mathcal{A}_i^2 (n_1^2 + n_2^2). \quad (2.10)$$

where the indices on E represent the number of the partial derivative. The indices a and i runs from 1 to 2. Note that E_0 and E_2 are positive semidefinite while E_1 can be either positive, negative or zero.

Let us define the scaling of $\vec{n}(x)$ as usual

$$\vec{n}^{(\lambda)}(x) = \vec{n}(\lambda x), \quad \partial_i \vec{n}^{(\lambda)}(x) = \lambda \partial'_i \vec{n}(\lambda x), \quad (2.11)$$

where ∂'_i stands for $\partial/\partial(\lambda x^i)$. On the other hand, the scaling of the gauge field differs from the dynamical one because we deal with the constant magnetic field and the gauge field is not dynamical. We define the scaling of the background gauge field as follows

$$\mathcal{A}_i^{(\lambda)}(x) = \lambda^{-1} \mathcal{A}_i(\lambda x). \quad (2.12)$$

Plugging Eq. (2.5) into this, we indeed see $\mathcal{A}_i^{(\lambda)}(x) = \mathcal{A}_i(x)$, and therefore the constant background magnetic field is not affected by the rescaling.

The λ dependence of the energy functional reads

$$\begin{aligned} e(\lambda) &= E \left[\vec{n}^{(\lambda)}(x) \right] \\ &= \int d^2x \left[\left(\frac{\partial n_a(\lambda x)}{\partial x^i} \right)^2 + 2e (\lambda^{-1} \mathcal{A}_i(\lambda x)) \varepsilon_{ab} \frac{\partial n_a(\lambda x)}{\partial x^i} n_b(\lambda x) \right. \\ &\quad \left. + e^2 (\lambda^{-1} \mathcal{A}_i(\lambda x))^2 (n_1(\lambda x)^2 + n_2(\lambda x)^2) \right] \\ &= \int \frac{d^2x'}{\lambda^2} \left[\left(\lambda \frac{\partial n_a(x')}{\partial x'^i} \right)^2 + 2e (\lambda^{-1} \mathcal{A}_i(x')) \varepsilon_{ab} \left(\lambda \frac{\partial n_a(x')}{\partial x'^i} \right) n_b(x') \right. \\ &\quad \left. + e^2 (\lambda^{-1} \mathcal{A}_i(x'))^2 (n_1(x')^2 + n_2(x')^2) \right] \\ &= E_2 + \lambda^{-2} E_1 + \lambda^{-4} E_0, \end{aligned} \quad (2.13)$$

where we have used $x'^j = \lambda x^j$. In order to see if this functional has a stationary point or not, we differentiate this with respect to λ to obtain

$$\frac{de(\lambda)}{d\lambda} = -2\lambda^{-3} E_1 - 4\lambda^{-5} E_0. \quad (2.14)$$

If $\vec{n}(x)$ is a static solution, this must be zero at $\lambda = 1$, provided

$$\delta \equiv E_1 + 2E_0 = 0. \quad (2.15)$$

As mentioned above $E_0 \geq 0$ whereas E_1 can be positive or negative. Hence, the system can successfully evade the Derrick's no-go theorem only for $E_1 < 0$.

2.3 $k = \pm 1$ lump solution and the selecting rule

Under the presence of nonzero background magnetic field $B \neq 0$, the charged field cannot be condensed in the vacuum. Therefore, the vacuum configuration should be $n_3 = \pm v$ with $n_1 + in_2 = 0$. Hence, the \mathbb{Z}_2 symmetry is spontaneously broken. We refer $n_3 = +v$ to the up vacuum while $n_3 = -v$ to the down vacuum.

Let us construct lump and anti-lump solutions. To this end, we make an axially symmetric Ansatz, given by

$$n_1 = v \frac{x}{r} \sin \Theta(r), \quad n_2 = v \frac{y}{r} \sin \Theta(r), \quad n_3 = v \cos \Theta(r), \quad (2.16)$$

with $r = \sqrt{x^2 + y^2}$. The lump with the winding number $k = +1$ satisfies the boundary condition $\Theta(0) = 0$ and $\Theta(\infty) = \pi$. Equivalently, this can be expressed as $n_3(0) = +v$ and $n_3(\infty) = -v$. Thus, this lump with $k = +1$ lives in the down vacuum $n_3 = -v$. Eq. (2.16) can also describe an anti-lump with $k = -1$ with the different boundary condition: $\Theta(0) = \pi$ and $\Theta(\infty) = 0$ or equivalently $n_3(0) = -v$ and $n_3(\infty) = +v$. Hence, the anti-lump lives in the up vacuum $n_3 = +v$. The lump in the down vacuum and the anti-lump in the up vacuum can be exchanged by $\Theta \rightarrow \pi - \Theta$ or $n_3 \rightarrow -n_3$.

Plugging this into Eq. (2.1), we find the Lagrangian written in terms of Θ as

$$\mathcal{L} = -\frac{B^2}{2} - v^2 \Theta'^2 - \frac{v^2(2 - eBr^2)^2}{4r^2} \sin^2 \Theta, \quad (2.17)$$

and the corresponding EOM reads

$$\Theta'' + \frac{\Theta'}{r} - \frac{(2 - eBr^2)^2}{4r^2} \sin \Theta \cos \Theta = 0, \quad (2.18)$$

where v disappears from EOM. Here, it is important to point out that EOM is not invariant under flipping the sign of eB . Note that the sign of eB is also important in the Derrick's scaling condition. Having the Ansatz (2.16), we can express E_0 and E_1 with respect to $\Theta(r)$ as

$$E_0 = \frac{\pi e^2 B^2 v^2}{2} \int_0^\infty dr r^3 \sin^2 \Theta, \quad (2.19)$$

$$E_1 = -2\pi e B v^2 \int_0^\infty dr r \sin^2 \Theta. \quad (2.20)$$

Both E_0 and E_1 can be nonzero for $B \neq 0$, thus the above scaling argument is meaningful only for the lump under a nonzero magnetic field. While $E_0 \geq 0$ is obvious from this expression, the sign of E_1 is the same as $-eB$. Since it has to be negative for Eq. (2.15) to be satisfied, we should choose $eB > 0$ for the Ansatz (2.16). More specifically, the lump in the down vacuum and the anti-lump in the up vacuum can only exist for $eB > 0$.

We can take another Ansatz with n_2 being replaced by $n_2 = -v \frac{y}{r} \sin \Theta$ in Eq. (2.16) while n_1 and n_3 are unchanged. We call this transformation ($n_2 \rightarrow -n_2$ up to $U(1)$ gauge transformation) the topological charge (TC) conjugation. This should be distinguished from the previous transformation $n_3 \rightarrow -n_3$ that flips not only the winding number but also

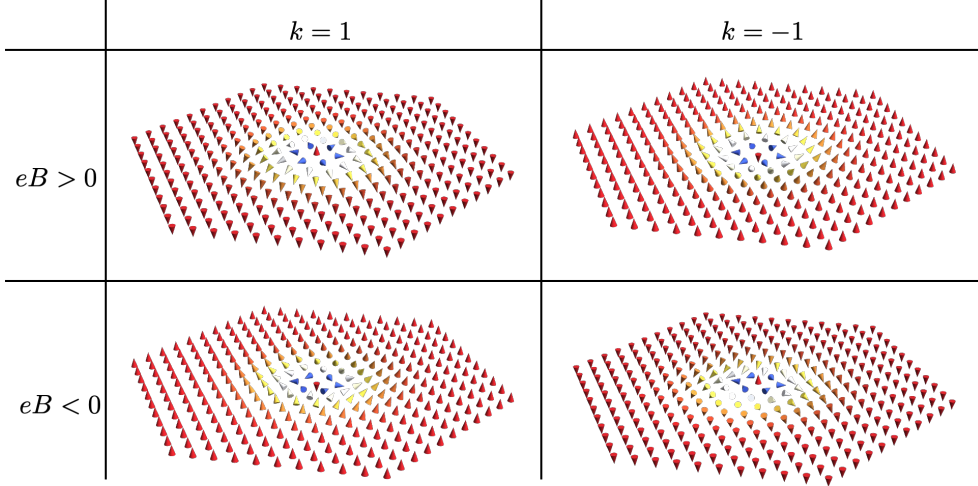


Figure 1. The selecting rule. The cones stand for \vec{n} . The cone upward is $n_3 = +v$ and that downward is $n_3 = -v$. The TC conjugation exchanges two diagonal entries, and two off-diagonal entries.

the vacuum. In contrast, the only lump charge is flipped by the TC conjugation. Indeed, the solution satisfying the boundary condition $\Theta(0) = 0$ and $\Theta(\infty) = \pi$ (equivalently $n_3(0) = +v$ and $n_3(\infty) = -v$) lives in the down vacuum and has the winding number $k = -1$, whereas that satisfying $\Theta(0) = \pi$ and $\Theta(\infty) = 0$ (equivalently $n_3(0) = -v$ and $n_3(\infty) = +v$) lives in the up vacuum and has the winding number $k = +1$. Note that the TC conjugation is identical to the normal charge conjugation $n_1 + in_2 \rightarrow n_1 - in_2$. The charge conjugation is also same as $e \rightarrow -e$. Therefore, Eqs. (2.17)–(2.20) remain correct with replacement $eB \rightarrow -eB$. Hence, we now need $eB < 0$ for realizing $E_1 < 0$. More specifically, the anti-lump in the down vacuum and the lump in the up vacuum can only exist for $eB < 0$.

The selecting rule and soliton-anti-soliton asymmetry This results in an interesting phenomenon. To clarify the lump solutions, we need to specify signs for the following three quantities: the first is the sign for the vacuum ($n_3 = \pm v$), the second is that for the magnetic field ($eB > 0$ or $eB < 0$), and the third is that for the topological charge ($k > 0$ or $k < 0$). If the background magnetic field is absent, we can put a lump or an anti-lump either in the up or down vacuum. However, when $B \neq 0$, there is a selecting rule that the lumps with positive topological charges ($k > 0$) can exist only when $\text{sign}(n_3) \cdot \text{sign}(eB) < 0$ is satisfied. Similarly, the anti-lumps with a negative topological charge ($k < 0$) can exist only when $\text{sign}(n_3) \cdot \text{sign}(eB) > 0$ holds. Hence, once the vacuum is chosen, one can select either lumps or anti-lumps by applying magnetic field. We call this phenomenon a violation of the TC conjugation, see Fig. 1.

Solutions for $B \neq 0$ can be only available by a numerical computation. However, asymptotic behavior can be analytically understood as follows. Since EOM includes eB (its mass dimension is 2), a solution will not have a size modulus. Indeed, the asymptotic

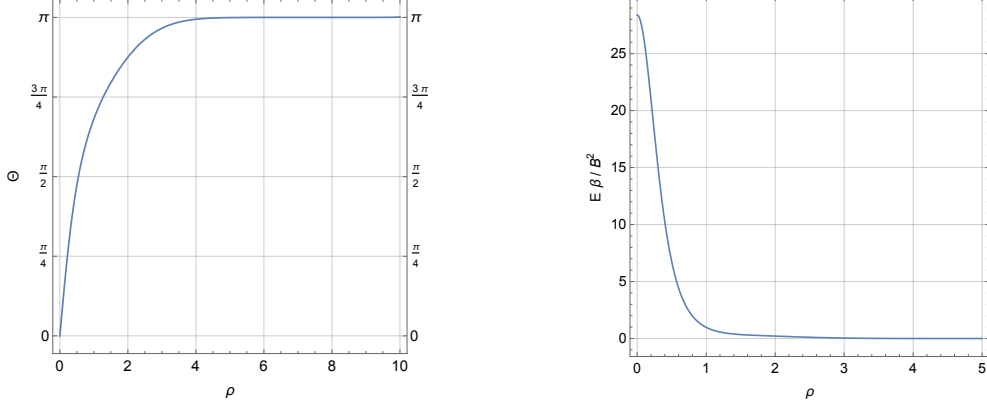


Figure 2. The numerical solution Θ and energy density of the single lump for $eB > 0$.

behavior should obey an exponential law rather than a power law. This can be easily verified by analyzing the linearized EOM for the fluctuation $\vartheta(r) = \pi - \Theta(r)$ at $r \gg 1/\sqrt{eB}$ as

$$-\vartheta'' + \frac{e^2 B^2 r^2}{4} \vartheta = 0, \quad \vartheta \propto \exp\left(-\frac{eB}{4} r^2\right), \quad (2.21)$$

with the expected decay length $1/\sqrt{eB}$.

Let us show the numerical solution. To this end, we first change the variable as $\rho = \sqrt{eB} r$. Then, EOM to be solved uniquely becomes

$$\Theta'' + \frac{\Theta'}{\rho} - \frac{(2 - \rho^2)^2}{4\rho^2} \sin \Theta \cos \Theta = 0, \quad (2.22)$$

where $\Theta' = \frac{d\Theta}{d\rho}$. The energy density and the mass are expressed as

$$\mathcal{E} = \frac{B^2}{\beta} \left[\Theta'^2 + \frac{(2 - \rho^2)^2}{4\rho^2} \sin^2 \Theta \right], \quad M = 2\pi v^2 \int \rho d\rho \mathcal{E}, \quad (2.23)$$

respectively. Here, we have introduced the dimensionless parameter for later convenience

$$\beta \equiv \frac{B}{ev^2}. \quad (2.24)$$

A numerical solution is shown in Fig. 2. Let us discuss features of this solution. First, we verify the Derrick's constraint in Eq. (2.15). With respect to the dimensionless coordinate, we have

$$E_0 = 2\pi v^2 \int_0^\infty d\rho \frac{\rho^3}{4} \sin^2 \Theta, \quad (2.25)$$

$$E_1 = -2\pi v^2 \int_0^\infty d\rho \rho \sin^2 \Theta, \quad (2.26)$$

and we numerically obtain $\delta/(2\pi v^2) = 3.32494 \times 10^{-7}$, thus Eq. (2.15) is satisfactory met within numerical accuracy. The mass of the lump is numerically evaluated as $M/(2\pi v^2) =$

3.62188. Note that this does not depend on eB . We also numerically determine the size $r_0 = \frac{0.544784}{\sqrt{eB}}$ of the lump from the condition $n_3(r_0) = 0$ ($\Theta(r_0) = \frac{\pi}{2}$). Hence, the magnetic flux inside the lump can be evaluated as $\Phi = \pi r_0^2 B \simeq 0.15 \times \frac{2\pi}{e}$.

We can compare our numerical solution with the BPS lump at $B = 0$, see Appendix A for some details. The mass of BPS lump is $M_{\text{BPS}}/(2\pi v^2) = 4$, therefore our numerical solution for $B \neq 0$ is slightly lighter than the BPS lump at $B = 0$. Furthermore, rough estimation of the fixed size of a BPS lump under the constant magnetic field B was given as $\tilde{r}_0 = \sqrt{\frac{2}{eB}}$ due to the magnetic flux quantization condition that the magnetic flux inside \tilde{r}_0 is $\tilde{\Phi} = \frac{2\pi}{e}$ [68]. Our numerical solution improves this, and the actual size is about 40% of \tilde{r}_0 , and the magnetic flux inside the lump is about 15% of $\tilde{\Phi}$.

2.4 Coaxial multiple lumps

We here quickly show the axially symmetric lumps with the winding number $k > 1$. To this end, we slightly change the Ansatz

$$n_1 = v \frac{\text{Re } z^k}{r^k} \sin \Theta(r), \quad n_2 = v \frac{\text{Im } z^k}{r^k} \sin \Theta(r), \quad n_3 = v \cos \Theta(r), \quad (2.27)$$

with $z \equiv x + iy$. The EOM reads

$$\Theta'' + \frac{\Theta'}{r} - \frac{(2k - eBr^2)^2}{4r^2} \sin \Theta \cos \Theta = 0, \quad (2.28)$$

and E_0 and E_1 are expressed as

$$E_0 = 2\pi v^2 \int_0^\infty d\rho \frac{\rho^3}{4} \sin^2 \Theta, \quad (2.29)$$

$$E_1 = -2k\pi v^2 \int_0^\infty d\rho \rho \sin^2 \Theta. \quad (2.30)$$

Here E_0 is independent of k while E_1 is proportional to k . The numerical solutions for $k = 1, 2, 3, 4, 5, 6$ are shown in Fig. 3. We numerically verify if the Derrick's condition is satisfied and find $\delta/(2\pi v^2) = -6.83875 \times 10^{-7}$, -1.17859×10^{-6} , -1.58112×10^{-6} , -1.63619×10^{-6} , -2.50128×10^{-6} for $k = 2, 3, 4, 5, 6$, respectively.

The lumps get fat as k increased. We numerically measure the radius r_0 for k as shown in Fig. 4 and find that it can be well approximated by $\frac{r_0}{\sqrt{eB}} = a\sqrt{k} + b$ with $a = 1.77$ and $b = -1.16$. Similarly, the mass is found as $\frac{M}{2\pi v^2} = c\sqrt{k} + d$ with $c = 4.86$ and $d = -1.18$. This suggests that the lumps are well described by a droplet model. Note that the lumps with $k > 1$ are empty in the sense that the energy densities at the cores are negligibly small.

3 Gauged lumps with dynamical gauge field in a magnetic field background

In this section, we consider a dynamical gauge field with a uniform background magnetic field. In Sec. 3.1, we introduce the dynamical gauge field. Then we explain the Derrick's

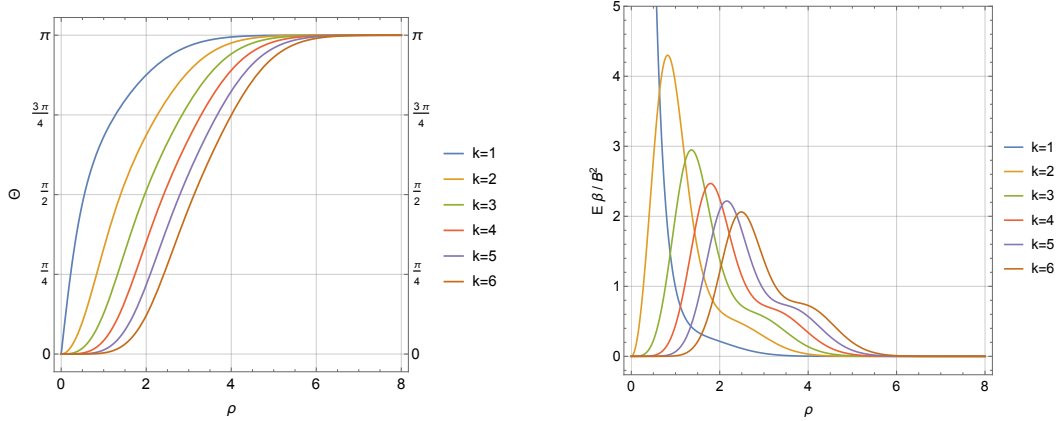


Figure 3. The numerical solutions Θ and energy densities for $k = 1, 2, 3, 4, 5$ with $eB > 0$.

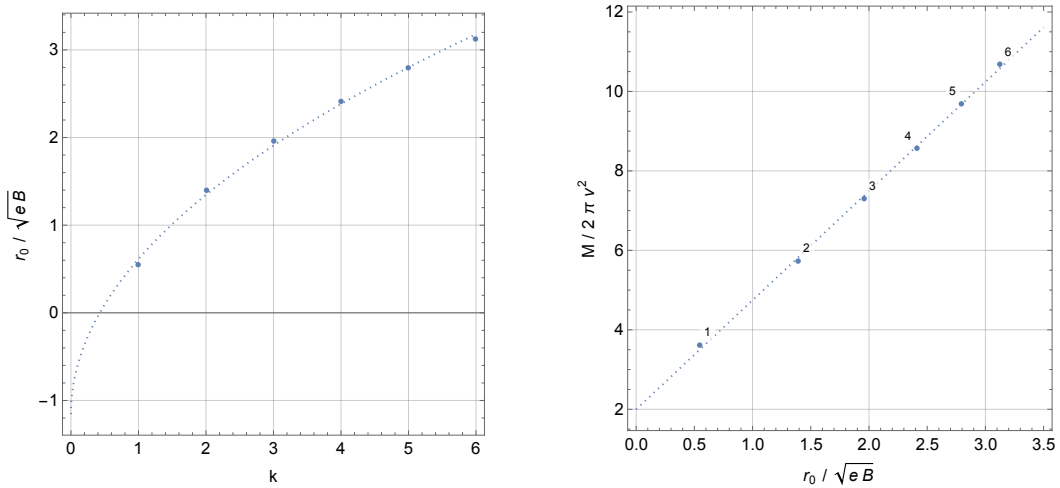


Figure 4. The numerical solutions Θ and energy densities for $k = 1, 2, 3, 4, 5, 6$ with $eB > 0$.

theorem in Sec. 3.2, and show the numerical solutions for the gauged lumps in Sec. 3.3. The anti-lumps and the soliton-anti-soliton asymmetry are explained in Sec. 3.4.

3.1 The model with dynamical gauge field

Next we deal with A_μ as a dynamical field. Since we are interested in the lumps under the constant magnetic field, we first need to decompose the gauge field into two parts as

$$A_\mu = \mathcal{A}_\mu + a_\mu, \quad (3.1)$$

where \mathcal{A}_μ is the nondynamical background gauge field given in Eq. (2.5) and a_μ is the dynamical gauge field.

3.2 Derrick's theorem

We modify the Derrick's scaling argument in the previous section to the case with a dynamical gauge field. The static and finite energies of the scalar field in the temporal gauge

$A_0 = 0$ are given by

$$\begin{aligned}
E[\vec{n}, a_\mu] &= \int d^2x \left(\frac{F_{12}^2}{2} - \frac{B^2}{2} + |D_i \vec{n}|^2 \right) \\
&= \int d^2x \left[\frac{(B + f_{12})^2}{2} - \frac{B^2}{2} \right. \\
&\quad \left. + |\partial_i \vec{n}|^2 + 2e(\mathcal{A}_i + a_i)\varepsilon_{ab}\partial_i n_a n_b + e^2(\mathcal{A}_i + a_i)^2(n_1^2 + n_2^2) \right], \quad (3.2)
\end{aligned}$$

respectively. We have subtracted $B^2/2$, and so that the energy remains finite. Let us decompose this into four parts as follows:

$$E[\vec{n}, a_\mu] = E_4 + E_2 + E_1 + E_0, \quad (3.3)$$

with

$$E_4 = \int d^2x \frac{f_{12}^2}{2}, \quad (3.4)$$

$$E_2 = \int d^2x [Bf_{12} + |\partial_i \vec{n}|^2 + 2ea_i\varepsilon_{ab}\partial_i n_a n_b + e^2 a_i^2(n_1^2 + n_2^2)], \quad (3.5)$$

$$E_1 = \int d^2x [2e\mathcal{A}_i\varepsilon_{ab}\partial_i n_a n_b + 2e^2\mathcal{A}_i a_i(n_1^2 + n_2^2)], \quad (3.6)$$

$$E_0 = \int d^2x e^2 \mathcal{A}_i^2(n_1^2 + n_2^2), \quad (3.7)$$

and $f_{12} = \partial_1 a_2 - \partial_2 a_1$.

Now we apply the Derrick's scaling argument to these as before. To this end, we use the same scaling laws Eqs. (2.11) and (2.12) for \vec{n} and \mathcal{A}_i , respectively. On the other hand, we adopt the standard scaling law for the dynamical gauge field a_μ as

$$a_i^{(\lambda)}(x) = \lambda a_i(\lambda x). \quad (3.8)$$

The λ dependence of the energy functional reads

$$e(\lambda) = E[\vec{n}^{(\lambda)}, a_\mu^{(\lambda)}] = \lambda^2 E_4 + \lambda^0 E_2 + \lambda^{-2} E_1 + \lambda^{-4} E_0. \quad (3.9)$$

In order to see if this functional has a stationary point or not, we differentiate this with respect to λ as

$$\frac{de(\lambda)}{d\lambda} = 2\lambda E_4 - 2\lambda^{-3} E_1 - 4\lambda^{-5} E_0. \quad (3.10)$$

If $\{\vec{n}(x), a_\mu\}$ is a static solution, this must be zero at $\lambda = 1$, provided

$$\delta' \equiv -E_4 + E_1 + 2E_0 = 0. \quad (3.11)$$

As before, E_1 can be either positive or negative whereas E_0 and E_4 are positive.

3.3 Multiple gauged lumps in the down vacuum with $eB > 0$

For a single lump, we make the following Ansatz

$$a_0 = 0, \quad a_1 = -\frac{Ba(r)}{2}y, \quad a_2 = \frac{Ba(r)}{2}x, \quad (3.12)$$

where a_μ is the dynamical gauge field as given in Eq. (3.1). Together with the background gauge field in Eq. (2.5), the full gauge field is given by

$$A_0 = 0, \quad A_1 = -\frac{B(1+a(r))}{2}y, \quad A_2 = \frac{B(1+a(r))}{2}x. \quad (3.13)$$

The mass dimension of $a(r)$ is zero. The magnetic field is given by

$$F_{12} = B(1+a) + \frac{Bra'}{2}. \quad (3.14)$$

We impose the profile function $a(r)$ to approach 0 as $r \rightarrow \infty$, so that the magnetic field asymptotically behaves as $F_{12} \rightarrow B$.

Plugging Eqs. (2.27) and (3.13) into Eq. (2.1), we find the reduced Lagrangian for Θ and a

$$\mathcal{L} = -\frac{B^2}{2} \left(1 + a + \frac{ra'}{2}\right)^2 - v^2 \Theta'^2 - v^2 \frac{(2k - eBr^2(1+a))^2}{4r^2} \sin^2 \Theta. \quad (3.15)$$

The corresponding EOMs are given by

$$\Theta'' + \frac{\Theta'}{r} - \frac{(2k - eBr^2(1+a))^2}{4r^2} \sin \Theta \cos \Theta = 0, \quad (3.16)$$

$$a'' + \frac{3a'}{r} + \frac{2ev^2(2k - eBr^2(1+a))}{Br^2} \sin^2 \Theta = 0. \quad (3.17)$$

Up to here in this subsection, the prime stands for a derivative in terms of the physical coordinate r .

For numerical analysis, let us rewrite these with respect to the dimensionless coordinate $\rho = \sqrt{eB}r$. Then we have

$$\Theta'' + \frac{\Theta'}{\rho} - \frac{(2k - \rho^2(1+a))^2}{4\rho^2} \sin \Theta \cos \Theta = 0, \quad (3.18)$$

$$a'' + \frac{3a'}{\rho} + \frac{2(2k - \rho^2(1+a))}{\beta\rho^2} \sin^2 \Theta = 0. \quad (3.19)$$

Now the prime indicates a derivative in terms of ρ . The EOMs include the dimensionless parameter β defined in Eq. (2.24). If we assume $a = 0$, Eq. (3.18) is identical to Eq. (2.22). On the other hand, Eq. (3.19) with $a = 0$ cannot be satisfied except for $\Theta = 0$ or π . Eq. (3.19) with $a = 0$ is approximately satisfied for a large B (or small e) such as $B \gg ev^2$. This is a reasonable condition for us to ignore the back reaction to the background gauge field.

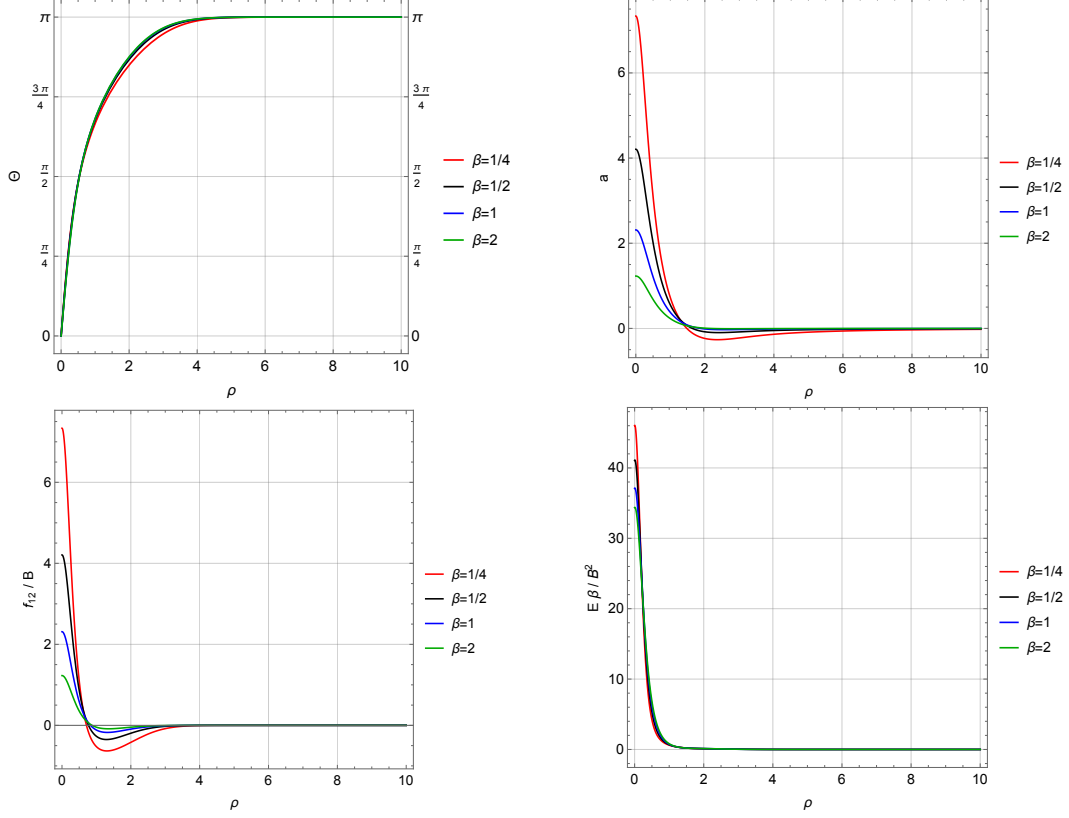


Figure 5. The numerical solution of $k = 1$ lump. Θ (top-left) and a (top-right). The back reaction f_{12} to the background magnetic field B (bottom-left) and energy density excited by the single lump. We take $\beta = \{1/4, 1/2, 1, 2\}$.

In what follows, we will concentrate on the lumps with $k > 0$ in the down vacuum with $eB > 0$. Namely, the boundary condition for Θ is $\Theta(0) = 0$ and $\Theta(\infty) = \pi$. The numerical solutions of $k = 1$ with different $\beta = \frac{1}{4}, \frac{1}{2}, 1$, and 2 are shown in Fig. 5. The anti-lumps with $k < 0$ in the negative vacuum with $eB > 0$ will separately be explained in Sec. 3.4. We first realize that back reaction to Θ is negligibly small irrespective of β , see the top-left panel. On the other hand, as can be seen in the top-right panel, the dynamical gauge field a_μ sensitively reacts to β . We also show the back reactions of the magnetic flux density and energy density

$$f_{12} = B \left(a + \frac{\rho}{2} a' \right), \quad (3.20)$$

$$\mathcal{E} = \frac{B^2}{\beta} \left[\frac{\beta}{2} \left\{ \left(1 + a + \frac{\rho}{2} a' \right)^2 - \frac{1}{2} \right\} + \Theta'^2 + \frac{(2k - \rho^2(1+a))^2}{4\rho^2} \sin^2 \Theta \right], \quad (3.21)$$

respectively, in the second row of Fig. 5. Note that the net magnetic flux is $F_{12} = B + f_{12}$ and we show f_{12} in Fig. 5. The magnetic flux is condensed at the center of the lump. It gets stronger than the background value B inside the lump core, and it reduces and changes its sign as going away from the lump, and asymptotically decays at spatial infinity. As expected, the greater β is, the smaller deformation of the profile a is. Namely, the back

$k = 1$	$\beta = 1/4$	$\beta = 1/2$	$\beta = 1$	$\beta = 2$	$\beta = \infty$
$\delta\Phi/(2\pi/e)$	-1.11	-0.400	-0.132	-0.0402	0
$M/(2\pi v^2)$	2.90	3.14	3.33	3.45	3.62
$\delta'/(2\pi B/e)$	-5.61×10^{-4}	-7.18×10^{-4}	-2.43×10^{-4}	-8.84×10^{-5}	—

Table 1. The quantitative properties of the $k = 1$ lump for $\beta = 1/2, 1,$ and 2 . We numerically evaluate changes of the net magnetic flux, the mass, and the Derrick's scaling condition $\delta' = 0$.

reaction tends to be small for the strong background magnetic field $B \gg ev^2$. This behavior can be explained as follows. Since $|n_1 + in_2| \neq 0$ at the edge of lump, the lump behaves as a superconducting ring and traps magnetic field in its inside, with the total magnetic field reduced from the background magnetic field because of superconductivity expelling it.

Let us quantitatively evaluate the numerical solutions. First, we measure a net change of the magnetic flux due to the single lump,

$$\delta\Phi = \int d^2x f_{12} = \frac{2\pi}{e} \int \rho d\rho \left(a + \frac{\rho}{2} a' \right). \quad (3.22)$$

This is shown for $\beta = \{\frac{1}{4}, \frac{1}{2}, 1, 2\}$ in Table 1. We find that $\delta\Phi$ is always negative, and thus the net background magnetic field is weakened under the presence of lump regardless of β .

Second, we measure the mass of the lump by

$$M = 2\pi v^2 \int \rho d\rho \left[\frac{\beta}{2} \left\{ \left(1 + a + \frac{\rho}{2} a' \right)^2 - 1 \right\} + \left\{ \Theta'^2 + \frac{(2k - \rho^2(1+a))^2}{4\rho^2} \sin^2 \Theta \right\} \right] \quad (3.23)$$

This is also summarised in Table 1.

Third, we calculate $E_4, E_1,$ and E_0 by

$$E_4 = \frac{2\pi B}{e} \int \rho d\rho \frac{1}{2} \left(a + \frac{\rho}{2} a' \right)^2, \quad (3.24)$$

$$E_1 = \frac{2\pi B}{e\beta} \int \rho d\rho \left(\frac{\rho^2 a}{2} - k \right) \sin^2 \Theta, \quad (3.25)$$

$$E_0 = \frac{2\pi B}{e\beta} \int \rho d\rho \frac{\rho^2}{4} \sin^2 \Theta, \quad (3.26)$$

and verify the scaling-stability condition $\delta' = 0$. The results are summarize in Table. 1 and they are satisfactory small.

Finally, we show the lumps with higher topological charges $k = 1, 2, 3, 4, 5, 6$ for $\beta = 1$ in Fig. 6. The profiles of Θ are qualitatively the same as those for the constant magnetic field shown in Fig. 3. The gauge field a and magnetic flux density f_{12} show plateaus inside the lump cores. The lumps are no longer empty and are filled by the magnetic field. These behaviors in f_{12} and \mathcal{E} are similar to those of well-known Abrikosov-Nielsen-Olsen vortices.

We also numerically solved EOMs for $\beta = 1/4, 1/2$ and $\beta = 2$, and the results are qualitatively the same as those for $\beta = 1$. As an example to see the similarity, we show the relation between the lump width r_0 and the winding number k for $\beta = \{1/4, 1/2, 1, 2\}$ in Fig. 7. We find it is well approximated by $\frac{r_0(k)}{\sqrt{eB}} = \sqrt{ak} + b$ as before. Namely, the lumps with magnetic fluxes behave as droplets.

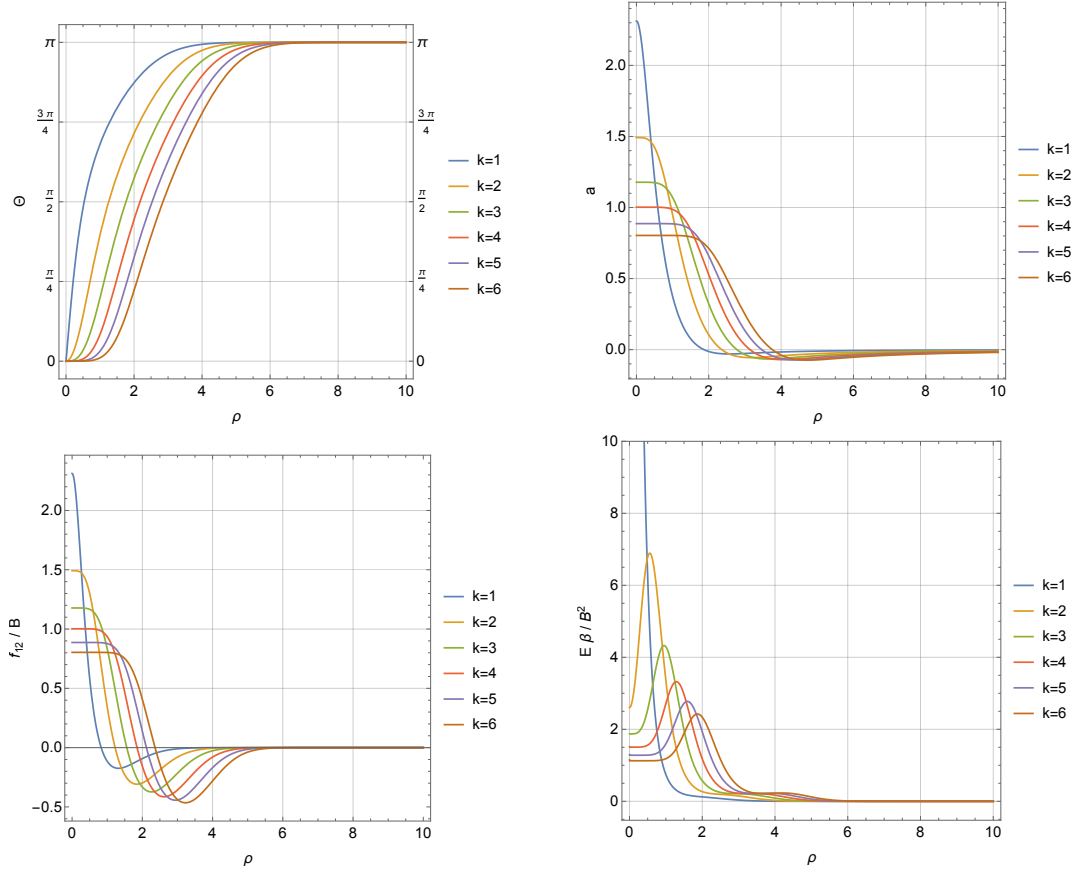


Figure 6. The axially symmetric lumps for $k = 1, 2, 3, 4, 5, 6$ for $\beta = 1$. Θ and a are shown in the top row, and f_{12} and \mathcal{E} are shown in the bottom row.

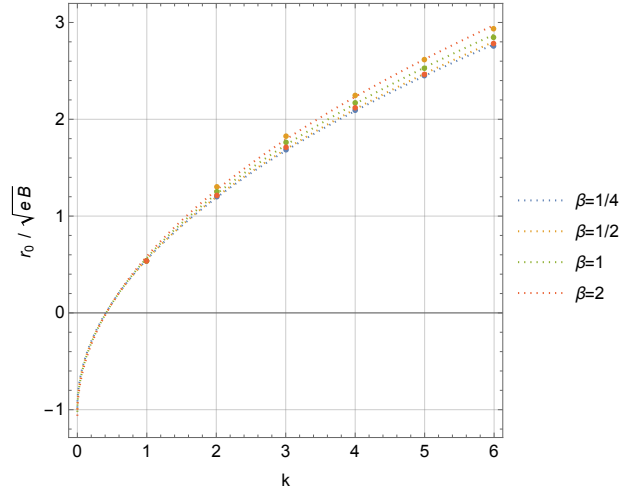


Figure 7. The relation between the lump size r_0 and the winding number k for $\beta = \{1/4, 1/2, 1, 2\}$.

3.4 Gauged anti-lumps in the down vacuum with $eB > 0$

Let us construct anti-lumps with the negative winding number $k < 0$ which do not exist in the case of nondynamical gauge field. For comparison, we take the same boundary condition as that taken in Sec. 3.3. Namely, we consider the anti-lumps in the negative vacuum and the background magnetic field is fixed by $eB > 0$.

We first remind that, in the treatment that the $U(1)$ gauge field is non-dynamical in Sec. 2, the Derrick's scaling condition (2.15) strictly prohibits the anti-lumps existing in the down vacuum with $eB > 0$. On the other hand, in the treatment that the $U(1)$ gauge field is dynamical, the scaling condition is relaxed as Eq. (3.11) due to the additional contribution by E_4 . Therefore, there would exist a room for the anti-lumps to exist in the model with dynamical gauge fields.

To verify this, we numerically solve EOMs in Eqs. (3.18) and (3.19) with $k < 0$ and the boundary condition $\Theta(0) = 0$ and $\Theta(\infty) = \pi$. Indeed, we numerically found non-singular anti-lump solutions.

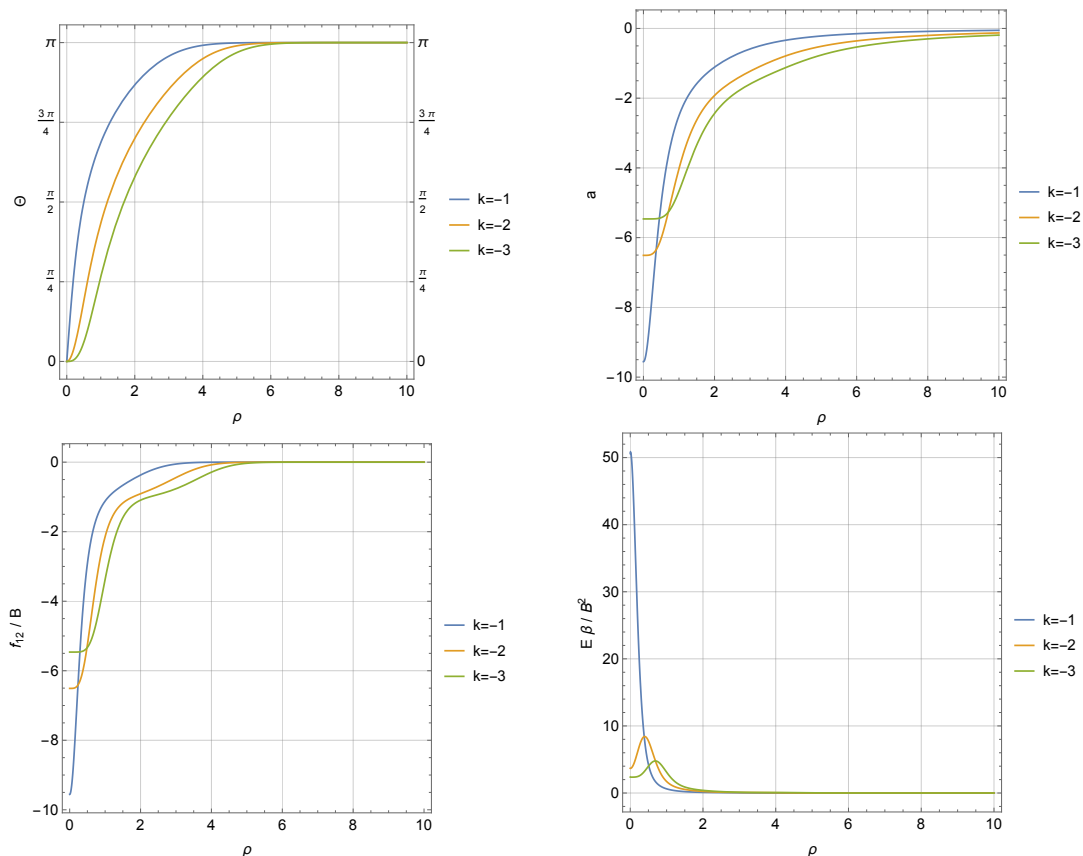


Figure 8. The axially symmetric lumps for $k = -1, -2, -3$ for $\beta = 1/4$ in the down vacuum. Θ and a are shown in the top row, and f_{12} and \mathcal{E} are shown in the bottom row.

As an example, we show the numerical solutions with $k = -1, -2, -3$ for $\beta = 1/4$ in Fig. 8. The anti-lumps trap the negative magnetic field in the cores which is opposite to the

background one $B(> 0)$. Unlike the case with $k > 0$, the back reaction f_{12} is everywhere negative.

The asymmetry between the lumps and anti-lumps in the model with the dynamical gauge field is more modest than that in the model without the dynamical field. However, the asymmetry does not disappear and remains as obviously seen in the EOMs in Eqs. (3.18) and (3.19). This can be also verified by our numerical solutions. Fig. 9 shows the energy densities (more explicitly, we show $\mathcal{E}\rho\beta/B^2$) of the $k = -1$ and $k = +1$ lumps under the same down vacuum with $\beta = 1/4$. We find that $k = -1$ lump has higher energy around its core and slightly lower at the outer bump. We numerically evaluate the mass of $k = -1$, and found $\frac{M}{2\pi v^2} = 2.97$ which is higher than $\frac{M}{2\pi v^2} = 2.90$ for $k = +1$, as shown in Table 1.

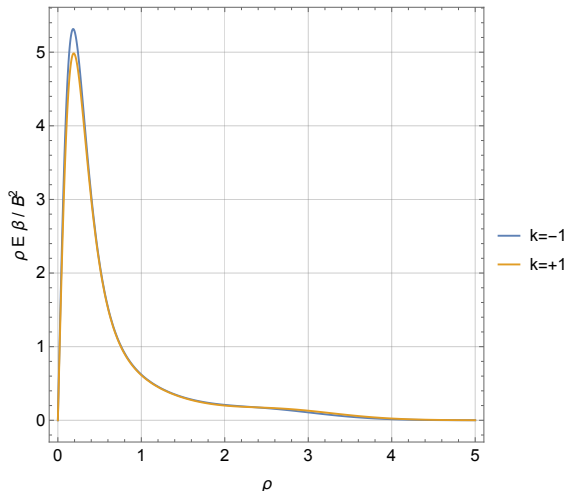


Figure 9. The comparison of energy densities of $k = -1$ and $k = +1$ for $\beta = 1/4$.

In conclusion, both the lumps and anti-lumps exist in the down vacuum with $eB > 0$, but the former is energetically favored than the latter. Intuitively, this reflects the fact that putting the soliton with the magnetic field opposite to the vacuum costs an energy than the soliton with the same magnetic field as the vacuum. The mass difference becomes larger as β is increased. In the limit $\beta \rightarrow \infty$ where the gauge field is non-dynamical, the anti-lumps tend to be singular and to be excluded from the system.

The same can be said for the up vacuum with $eB > 0$ or $eB < 0$ by appropriately exchanging the lump and anti-lump.

4 Summary and discussion

In this paper, we have worked out stable lumps in a gauged $O(3)$ model without any potential term coupled with a (non)dynamical $U(1)$ gauge field. We have found that the gauged-lumps without a potential term can be made stable by putting them in a uniform magnetic field, irrespective of whether the gauge field is dynamical or not. In the case

of the non-dynamical gauge field, we have found that only either of lumps or anti-lumps stably exists depending on the sign of the background magnetic field, and the other is unstable to shrink to be singular. The case of nondynamical gauge field resemble magnetic Skyrmions in chiral magnets. We have also constructed coaxial lumps with higher winding number k , whose size and mass are proportional to \sqrt{k} up to a constant shift, implying that they behave as droplets. On the other hand, in the case of the dynamical gauge field, we have found that both the lumps and anti-lumps stably exist with different masses; the lighter (heavier) one corresponds to the (un)stable one in the case of the nondynamical gauge field. The lumps behave as superconducting rings, trapping magnetic fields in their interiors. The total magnetic fluxes are reduced from the background magnetic field because of superconductivity.

In this paper, we have discussed only axially symmetric configurations for multiple lump states. The next step should be to investigate separated configurations and study interaction among them. Since the profile of a single lump exponentially decays, the interaction would be exponentially suppressed like vortices in superconductors. In particular, we expect a repulsive force between two lumps and the existence of a lattice as the case of magnetic Skyrmions [37–40, 42]¹. This is quite important for an application to domain-wall Skyrmions in QCD under strong magnetic field.

One natural generalization of the current work is the $\mathbb{C}P^{N-1}$ model. From a theoretical point of view, a naive question is if one $U(1)$ gauging is enough or $U(1)^{N-1}$ gauging is necessary for the stability of $\mathbb{C}P^{N-1}$ lumps. From a physical point of view, such a $U(1)$ gauged $\mathbb{C}P^2$ model appears on a chiral soliton with three flavors (up, down and strange quarks) in which case $\mathbb{C}P^2$ lumps are $SU(3)$ Skyrmions from the bulk point of view. The $U(1)$ gauged $\mathbb{C}P^2$ model also appears [74–76] on the worldsheet of a non-Abelian vortex in dense QCD [11, 77–81] in which case lumps are sigma model instantons viewed as Yang-Mills instantons from the bulk [82].

Our model would have an impact on production of topological solitons. During a phase transition accompanied with a spontaneous symmetry breaking, topological solitons are in general created by the Kibble-Zurek-mechanism. Usually the numbers of solitons and anti-solitons created in this way are the same. If we consider such a phase transition in our model, the background magnetic field works as a bias leading to an asymmetry between the lumps or anti-lumps. Hence, this suggests a new impact on solitogenesis and might be useful for baryogenesis in early Universe.

Acknowledgments

YA is grateful for the hospitality at the Department of Physics of Yamagata University, where this work was initiated. This work is supported in part by JSPS KAKENHI [Grants No. JP23KJ1881 (YA), No. JP22H01221 (ME and MN)] and the WPI program “Sustainability with Knotted Chiral Meta Matter (SKCM²)” at Hiroshima University (ME and MN).

¹However, the interaction between magnetic Skyrmions was polynomial like [42].

A A BPS lump for $B = 0$

Here let us quickly recall the analytic solution for $B = 0$. The EOM reduces to one for a usual $\mathbb{C}P^1$ lump, and its analytic solution is available as

$$\frac{n_3(r)}{v} = \cos \Theta(r) = \frac{a^2 - r^2}{a^2 + r^2}. \quad (\text{A.1})$$

Here, a is so called size modulus. As usual, we define the size r_0 of lump by $n_3(r_0) = 0$. Clearly, we have $r_0 = a$. This solution satisfies the boundary condition $\cos \Theta(0) = 0$ and $\cos \Theta(\infty) = \pi$ ($n_3(0) = v$ and $n_3(\infty) = -v$). The asymptotic behavior at $r \rightarrow \infty$ is power law as $\frac{n_3}{v} = -1 + \frac{2a^2}{r^2} + \dots$.

Let C be a closed curve on which $n_3 = 0$, and D be the interior of C . The $U(1)$ is spontaneously and maximally broken around $|n_1 + in_2| = v$. Thus, the closed curve C is a superconducting ring, and there is a persistent current along it. Let us write $n_1 + in_2 = ve^{i\psi}$ on C . The configuration of the gauge field along C is determined by minimizing the gradient energy $|D_\alpha(n_1 + in_2)|^2 = 0$, yielding $\partial_\alpha \psi = eA_\alpha$. Then, we have a flux (and area) quantization on D :

$$BS_D = \int_D d^2x B = \oint_C dx^i A_i = \frac{1}{e} \oint_C dx^i \partial_i \psi = \frac{2\pi}{e} \quad (\text{A.2})$$

with the area S_D of D . This gives a constraint among the lump moduli. For a single BPS lump with $n_3 = v(a^2 - r^2)/(a^2 + r^2)$. Thus, the size of D bounded by $n_3 = 0$ is $r = a$, and the flux quantization implies a quantization of the size $a = \sqrt{2/eB}$.

References

- [1] R. Rajaraman, *Solitons and Instantons: An Introduction to Solitons and Instantons in Quantum Field Theory*. North-Holland Personal Library, 1987.
- [2] N. S. Manton and P. Sutcliffe, *Topological solitons*, Cambridge Monographs on Mathematical Physics. Cambridge University Press, 2004, [10.1017/CBO9780511617034](https://doi.org/10.1017/CBO9780511617034).
- [3] Y. M. Shnir, *Magnetic Monopoles*, Text and Monographs in Physics. Springer, Berlin/Heidelberg, 2005, [10.1007/3-540-29082-6](https://doi.org/10.1007/3-540-29082-6).
- [4] M. Eto, Y. Isozumi, M. Nitta, K. Ohashi and N. Sakai, *Solitons in the Higgs phase: The Moduli matrix approach*, *J. Phys. A* **39** (2006) R315 [[hep-th/0602170](https://arxiv.org/abs/hep-th/0602170)].
- [5] T. Vachaspati, *Kinks and domain walls: An introduction to classical and quantum solitons*. Cambridge University Press, 4, 2010, [10.1017/CBO9780511535192](https://doi.org/10.1017/CBO9780511535192).
- [6] E. J. Weinberg and P. Yi, *Magnetic Monopole Dynamics, Supersymmetry, and Duality*, *Phys. Rept.* **438** (2007) 65 [[hep-th/0609055](https://arxiv.org/abs/hep-th/0609055)].
- [7] M. Shifman and A. Yung, *Supersymmetric solitons*, Cambridge Monographs on Mathematical Physics. Cambridge University Press, 5, 2009, [10.1017/CBO9780511575693](https://doi.org/10.1017/CBO9780511575693).
- [8] M. Dunajski, *Solitons, instantons, and twistors*, Oxford Graduate Texts In Mathematics. Oxford University Press, U.S.A., 2010.

- [9] E. J. Weinberg, *Classical solutions in quantum field theory: Solitons and Instantons in High Energy Physics*, Cambridge Monographs on Mathematical Physics. Cambridge University Press, 9, 2012, [10.1017/CBO9781139017787](https://doi.org/10.1017/CBO9781139017787).
- [10] Y. M. Shnir, *Topological and Non-Topological Solitons in Scalar Field Theories*. Cambridge University Press, 7, 2018, [10.1017/9781108555623](https://doi.org/10.1017/9781108555623).
- [11] M. Eto, Y. Hirono, M. Nitta and S. Yasui, *Vortices and Other Topological Solitons in Dense Quark Matter*, *PTEP* **2014** (2014) 012D01 [[1308.1535](https://arxiv.org/abs/1308.1535)].
- [12] T. W. B. Kibble, *Topology of Cosmic Domains and Strings*, *J. Phys. A* **9** (1976) 1387.
- [13] A. Vilenkin, *Cosmic Strings and Domain Walls*, *Phys. Rept.* **121** (1985) 263.
- [14] M. Hindmarsh and T. Kibble, *Cosmic strings*, *Rept. Prog. Phys.* **58** (1995) 477 [[hep-ph/9411342](https://arxiv.org/abs/hep-ph/9411342)].
- [15] A. Vilenkin and E. S. Shellard, *Cosmic Strings and Other Topological Defects*. Cambridge University Press, 7, 2000.
- [16] T. Vachaspati, L. Pogosian and D. Steer, *Cosmic Strings*, *Scholarpedia* **10** (2015) 31682 [[1506.04039](https://arxiv.org/abs/1506.04039)].
- [17] N. D. Mermin, *The topological theory of defects in ordered media*, *Rev. Mod. Phys.* **51** (1979) 591.
- [18] G. E. Volovik, *The Universe in a helium droplet*, International Series of Monographs on Physics. Oxford Scholarship Online, 2009, [10.1093/acprof:oso/9780199564842.001.0001](https://doi.org/10.1093/acprof:oso/9780199564842.001.0001).
- [19] L. Pismen, *Vortices in Nonlinear Fields: From Liquid Crystals to Superfluids, from Non-Equilibrium Patterns to Cosmic Strings*, International Series of Monographs on Physics. Clarendon Press, 1999.
- [20] B. V. Svistunov, E. S. Babaev and N. V. Prokof'ev, *Superfluid States of Matter*, Cambridge Monographs on Mathematical Physics. CRC Press, 2015, [10.1201/b18346](https://doi.org/10.1201/b18346).
- [21] Y. Kawaguchi and M. Ueda, *Spinor Bose-Einstein condensates*, *Phys. Rept.* **520** (2012) 253.
- [22] G. H. Derrick, *Comments on nonlinear wave equations as models for elementary particles*, *J. Math. Phys.* **5** (1964) 1252.
- [23] T. H. R. Skyrme, *A Nonlinear field theory*, *Proc. Roy. Soc. Lond. A* **260** (1961) 127.
- [24] T. H. R. Skyrme, *A Unified Field Theory of Mesons and Baryons*, *Nucl. Phys.* **31** (1962) 556.
- [25] J. Gladikowski and M. Hellmund, *Static solitons with nonzero Hopf number*, *Phys. Rev. D* **56** (1997) 5194 [[hep-th/9609035](https://arxiv.org/abs/hep-th/9609035)].
- [26] L. D. Faddeev and A. J. Niemi, *Knots and particles*, *Nature* **387** (1997) 58 [[hep-th/9610193](https://arxiv.org/abs/hep-th/9610193)].
- [27] R. A. Battye and P. M. Sutcliffe, *Knots as stable soliton solutions in a three-dimensional classical field theory.*, *Phys. Rev. Lett.* **81** (1998) 4798 [[hep-th/9808129](https://arxiv.org/abs/hep-th/9808129)].
- [28] A. M. Polyakov and A. A. Belavin, *Metastable States of Two-Dimensional Isotropic Ferromagnets*, *JETP Lett.* **22** (1975) 245.
- [29] A. A. Bogolubskaya and I. L. Bogolubsky, *Stationary Topological Solitons in the Two-dimensional Anisotropic Heisenberg Model With a Skyrme Term*, *Phys. Lett. A* **136** (1989) 485.

- [30] A. A. Bogolyubskaya and I. L. Bogolyubsky, *ON STATIONARY TOPOLOGICAL SOLITONS IN TWO-DIMENSIONAL ANISOTROPIC HEISENBERG MODEL*, *Lett. Math. Phys.* **19** (1990) 171.
- [31] B. M. A. G. Piette, B. J. Schroers and W. J. Zakrzewski, *Multi - solitons in a two-dimensional Skyrme model*, *Z. Phys. C* **65** (1995) 165 [[hep-th/9406160](#)].
- [32] T. Weidig, *The Baby skyrme models and their multiskyrmions*, *Nonlinearity* **12** (1999) 1489 [[hep-th/9811238](#)].
- [33] R. A. Leese, *Q lumps and their interactions*, *Nucl. Phys. B* **366** (1991) 283.
- [34] E. Abraham, *Nonlinear sigma models and their Q lump solutions*, *Phys. Lett. B* **278** (1992) 291.
- [35] A. Bogdanov and D. Yablonskii, *Thermodynamically stable vortices in magnetically ordered crystals. The mixed state of magnets*, *Sov. Phys. JETP* **68** (1989) 101.
- [36] A. Bogdanov, *New localized solutions of the nonlinear field equations*, *JETP Lett.* **62** (1995) 247.
- [37] U. K. Rossler, A. N. Bogdanov and C. Pfleiderer, *Spontaneous skyrmion ground states in magnetic metals*, *Nature* **442** (2006) 797.
- [38] S. Mühlbauer, B. Binz, F. Jonietz, C. Pfleiderer, A. Rosch, A. Neubauer et al., *Skyrmion lattice in a chiral magnet*, *Science* **323** (2009) 915.
- [39] X. Z. Yu, Y. Onose, N. Kanazawa, J. H. Park, J. H. Han, Y. Matsui et al., *Real-space observation of a two-dimensional skyrmion crystal*, *Nature* **465** (2010) 901.
- [40] J. H. Han, J. Zang, Z. Yang, J.-H. Park and N. Nagaosa, *Skyrmion Lattice in Two-Dimensional Chiral Magnet*, *Phys. Rev. B* **82** (2010) 094429.
- [41] B. Barton-Singer, C. Ross and B. J. Schroers, *Magnetic Skyrmions at Critical Coupling*, *Commun. Math. Phys.* **375** (2020) 2259 [[1812.07268](#)].
- [42] C. Ross, N. Sakai and M. Nitta, *Skyrmion interactions and lattices in chiral magnets: analytical results*, *JHEP* **02** (2021) 095 [[2003.07147](#)].
- [43] Y. Amari and M. Nitta, *Chiral magnets from string theory*, *JHEP* **11** (2023) 212 [[2307.11113](#)].
- [44] I. Dzyaloshinskii, *A Thermodynamic Theory of ‘Weak’ Ferromagnetism of Antiferromagnetics*, *J. Phys. Chem. Solids* **4** (1958) 241.
- [45] T. Moriya, *Anisotropic Superexchange Interaction and Weak Ferromagnetism*, *Phys. Rev.* **120** (1960) 91.
- [46] B. J. Schroers, *Gauged Sigma Models and Magnetic Skyrmions*, *SciPost Phys.* **7** (2019) 030 [[1905.06285](#)].
- [47] C. Ross and M. Nitta, *Domain-wall skyrmions in chiral magnets*, *Phys. Rev. B* **107** (2023) 024422 [[2205.11417](#)].
- [48] Y. Akagi, Y. Amari, N. Sawado and Y. Shnir, *Isolated skyrmions in the CP^2 nonlinear sigma model with a Dzyaloshinskii-Moriya type interaction*, *Phys. Rev. D* **103** (2021) 065008 [[2101.10566](#)].
- [49] Y. Amari, Y. Akagi, S. B. Gudnason, M. Nitta and Y. Shnir, *CP^2 skyrmion crystals in an*

- SU(3) magnet with a generalized Dzyaloshinskii-Moriya interaction*, *Phys. Rev. B* **106** (2022) L100406 [2204.01476].
- [50] Y. J. Lin, R. L. Compton, K. Jiménez-García, J. V. Porto and I. B. Spielman, *Synthetic magnetic fields for ultracold neutral atoms*, *Nature* **462** (2009) 628.
- [51] N. Goldman, G. Juzeliūnas, P. Öhberg and I. B. Spielman, *Light-induced gauge fields for ultracold atoms*, *Rept. Prog. Phys.* **77** (2014) 126401 [1308.6533].
- [52] T. Kawakami, T. Mizushima and K. Machida, *Textures of $f = 2$ spinor bose-einstein condensates with spin-orbit coupling*, *Phys. Rev. A* **84** (2011) 011607.
- [53] T. Kawakami, T. Mizushima, M. Nitta and K. Machida, *Stable Skyrmions in SU(2) Gauged Bose-Einstein Condensates*, *Phys. Rev. Lett.* **109** (2012) 015301 [1204.3177].
- [54] B. J. Schroers, *Bogomolny solitons in a gauged O(3) sigma model*, *Phys. Lett. B* **356** (1995) 291 [hep-th/9506004].
- [55] B. J. Schroers, *The Spectrum of Bogomol'nyi solitons in gauged linear sigma models*, *Nucl. Phys. B* **475** (1996) 440 [hep-th/9603101].
- [56] J. M. Baptista, *Vortex equations in Abelian gauged sigma-models*, *Commun. Math. Phys.* **261** (2006) 161 [math/0411517].
- [57] M. Nitta and W. Vinci, *Decomposing Instantons in Two Dimensions*, *J. Phys. A* **45** (2012) 175401 [1108.5742].
- [58] D. E. Kharzeev, *Topology, magnetic field, and strongly interacting matter*, *Ann. Rev. Nucl. Part. Sci.* **65** (2015) 193 [1501.01336].
- [59] V. A. Miransky and I. A. Shovkovy, *Quantum field theory in a magnetic field: From quantum chromodynamics to graphene and Dirac semimetals*, *Phys. Rept.* **576** (2015) 1 [1503.00732].
- [60] J. O. Andersen, W. R. Naylor and A. Tranberg, *Phase diagram of QCD in a magnetic field: A review*, *Rev. Mod. Phys.* **88** (2016) 025001 [1411.7176].
- [61] A. Yamamoto, *Overview of external electromagnetism and rotation in lattice QCD*, *Eur. Phys. J. A* **57** (2021) 211 [2103.00237].
- [62] G. Cao, *Recent progresses on QCD phases in a strong magnetic field: views from Nambu–Jona-Lasinio model*, *Eur. Phys. J. A* **57** (2021) 264 [2103.00456].
- [63] S. Iwasaki, M. Oka and K. Suzuki, *A review of quarkonia under strong magnetic fields*, *Eur. Phys. J. A* **57** (2021) 222 [2104.13990].
- [64] D. T. Son and M. A. Stephanov, *Axial anomaly and magnetism of nuclear and quark matter*, *Phys. Rev. D* **77** (2008) 014021 [0710.1084].
- [65] M. Eto and M. Nitta, *Quantum nucleation of topological solitons*, *JHEP* **09** (2022) 077 [2207.00211].
- [66] M. Eto, K. Hashimoto and T. Hatsuda, *Ferromagnetic neutron stars: axial anomaly, dense neutron matter, and pionic wall*, *Phys. Rev. D* **88** (2013) 081701 [1209.4814].
- [67] T. Brauner and N. Yamamoto, *Chiral Soliton Lattice and Charged Pion Condensation in Strong Magnetic Fields*, *JHEP* **04** (2017) 132 [1609.05213].
- [68] M. Eto, K. Nishimura and M. Nitta, *How baryons appear in low-energy QCD: Domain-wall Skyrmion phase in strong magnetic fields*, [2304.02940](#).

- [69] M. Eto, K. Nishimura and M. Nitta, *Phase diagram of QCD matter with magnetic field: domain-wall Skyrmion chain in chiral soliton lattice*, *JHEP* **12** (2023) 032 [[2311.01112](#)].
- [70] M. Eto, K. Nishimura and M. Nitta, *Domain-wall Skyrmion phase in a rapidly rotating QCD matter*, *JHEP* **01** (2024) 019 [[2310.17511](#)].
- [71] M. Nitta, *Correspondence between Skyrmions in 2+1 and 3+1 Dimensions*, *Phys. Rev. D* **87** (2013) 025013 [[1210.2233](#)].
- [72] M. Nitta, *Matryoshka Skyrmions*, *Nucl. Phys. B* **872** (2013) 62 [[1211.4916](#)].
- [73] S. B. Gudnason and M. Nitta, *Domain wall Skyrmions*, *Phys. Rev. D* **89** (2014) 085022 [[1403.1245](#)].
- [74] W. Vinci, M. Cipriani and M. Nitta, *Spontaneous Magnetization through Non-Abelian Vortex Formation in Rotating Dense Quark Matter*, *Phys. Rev. D* **86** (2012) 085018 [[1206.3535](#)].
- [75] Y. Hirono and M. Nitta, *Anisotropic optical response of dense quark matter under rotation: Compact stars as cosmic polarizers*, *Phys. Rev. Lett.* **109** (2012) 062501 [[1203.5059](#)].
- [76] C. Chatterjee and M. Nitta, *Aharonov-Bohm Phase in High Density Quark Matter*, *Phys. Rev. D* **93** (2016) 065050 [[1512.06603](#)].
- [77] A. P. Balachandran, S. Dugal and T. Matsuura, *Semi-superfluid strings in high density QCD*, *Phys. Rev. D* **73** (2006) 074009 [[hep-ph/0509276](#)].
- [78] E. Nakano, M. Nitta and T. Matsuura, *Non-Abelian strings in high density QCD: Zero modes and interactions*, *Phys. Rev. D* **78** (2008) 045002 [[0708.4096](#)].
- [79] M. Eto and M. Nitta, *Color Magnetic Flux Tubes in Dense QCD*, *Phys. Rev. D* **80** (2009) 125007 [[0907.1278](#)].
- [80] M. Eto, E. Nakano and M. Nitta, *Effective world-sheet theory of color magnetic flux tubes in dense QCD*, *Phys. Rev. D* **80** (2009) 125011 [[0908.4470](#)].
- [81] M. Eto, M. Nitta and N. Yamamoto, *Instabilities of Non-Abelian Vortices in Dense QCD*, *Phys. Rev. Lett.* **104** (2010) 161601 [[0912.1352](#)].
- [82] M. Eto, Y. Isozumi, M. Nitta, K. Ohashi and N. Sakai, *Instantons in the Higgs phase*, *Phys. Rev. D* **72** (2005) 025011 [[hep-th/0412048](#)].